

BACKGROUND CALCULATIONS FOR THE HIGH ENERGY BEAM TRANSPORT REGION OF THE EUROPEAN SPALLATION SOURCE

R. J. Barlow*, A. M. Toader, University of Huddersfield, UK
 L. Tchelidze, ESS, Lund, Sweden
 H. D. Thomsen, ISA, Aarhus, Denmark

Abstract

Expected backgrounds in the final accelerator-to-target region of the European Spallation Source, to be built in Lund, Sweden, have been calculated using the MCNPX program. We consider the effects of losses from the beam, both along the full length and localised at the bending magnets, and also backsplash from the target. The prompt background is calculated, and also the residual dose, as a function of time, arising from activation of the beam components. Activation of the air is also determined. The model includes the focussing and rasterising magnets, and shows the effects of the concrete walls of the tunnel. We give the implications for the design and operation of the accelerator.

THE PROBLEM

The European Spallation Source (ESS) will shortly begin construction at Lund, Sweden [1]. The final high energy beam transport (HEBT) region is some 50 m long, keeping the possibility open for upgrades, and the proton beam travels through it at full energy. The region is also close to the target monolith. Both these sources have the potential to produce significant background radiation in this region, with consequences for apparatus and access.

We use the MCNPX code [2] to simulate the interactions. Because the effects considered are due to a very small fraction of a very large number of interactions, significant computation time is needed, even though variance reduction techniques are used. The default cross sections are used, however the neutron energy-to-dose conversion factor is modified by a standard form in use by at ESS.

We evaluate effects due to two sources: (i) losses from the beam pipe, normalised to the nominal maximum loss of 1 W/m, between 60 m and 17 m upstream of the target, and (ii) backsplash from the target, normalised to a power of 5 MW. For both of these we calculate (i) the prompt dose due to neutrons and photons produced during operation and (ii) the delayed dose due to photons from activated nuclei, assuming 100 hours of continuous running followed a 4 hour delay. The proton energy was taken as 2 GeV.

We have adapted the standard ESS MCNP geometry deck (Target Station Monolith 13/03/18) as shown in Fig. 1, by the addition of

- A stainless steel beam pipe 2 mm thick and 60 mm in radius, from the final dog-leg to the target monolith
- 6 Quadrupole focussing magnets, with iron yokes and copper windings shown in Fig. 2

- 8 small rectangular raster dipole magnets (four horizontal and four vertical), also of iron and copper, shown (not to scale) in the same figure. In this region the beam pipe is ceramic (taken as Al_2O_3), 8 mm thick and 40 mm in radius
- A concrete wall, between the last magnet and the monolith, 3 m wide, 3.5 m high and 2 m thick. Here the steel beam pipe is 20 mm in radius leaving 3 mm between the pipe and the concrete. Variations in wall thickness were considered.
- A concrete wall to the tunnel, 1 m thick. This can act as a funnel for backsplash neutrons.

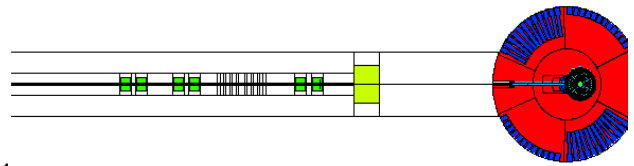


Figure 1: The HEBT line. (Construction lines are shown).

For the activation we consider the isotopes shown in Table 1, which have relevant half-lives and occur in non-negligible amounts in the components

Table 1: Isotopes

Isotope	E_γ MeV	$\tau_{1/2}$	Parent	Found in
^{57}Co	0.12	272 d	$^{58}Ni(n, d)$	Steel
^{58}Co	0.81	71 d	$^{58}Ni(n, p)$	Steel
^{60}Co	1.1, 1.3	5.3 y	$^{63}Cu(n, \alpha)$	Copper
^{54}Mn	0.85	312 d	$^{54}Fe(n, p)$	Iron+Steel
^{56}Mn	0.83, 1.8	2.6 h	$^{55}Mn(n, \gamma)$	Steel
^{22}Na	0.51, 1.3	2.6 y	$^{23}Na(n, 2n)$	Concrete
^{24}Na	1.4, 2.8	15 h	$^{23}Na(n, \gamma)$, $^{27}Al(n, \alpha)$	Concrete, Ceramic

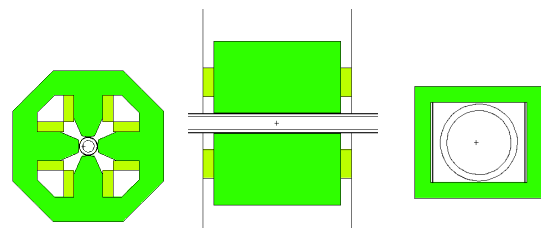


Figure 2: Quad and raster magnets.

* R.Barlow@hud.ac.uk

RESULTS

Results are typically obtained by simulating 1.25 M source protons in 25 separate jobs, the results of which were combined. For backscatter simulations (which are slower than beam losses) this takes around 12 hours. Variance reduction was achieved by ascribing greater importance to geometrical regions between the target and the beam entrance and results with a quoted error of a few percent were achieved.

Prompt Rates from the Target

Fig. 3 shows the neutron flux produced from backscattering from the target, considering a vertical slice through the beam axis. Note the difference in scales on this plot: it shows the 55m length of the HEBT horizontally and the 8m height of the tunnel plus surrounding concrete vertically. The shielding wall is made from standard ‘ordinary’ concrete [3] with a density of 2.35g/cm^3 .

The greatest predicted flux value is 5×10^{11} neutrons per square cm per second, though this falls off very rapidly, particularly as a result of shielding by the 2 m thick neutron wall (at $z=-16.7$ m from the target as shown in Fig. 1). Some rescattering inside the tunnel from the surrounding wall is observed, but we find that very little flux emerges outside it.

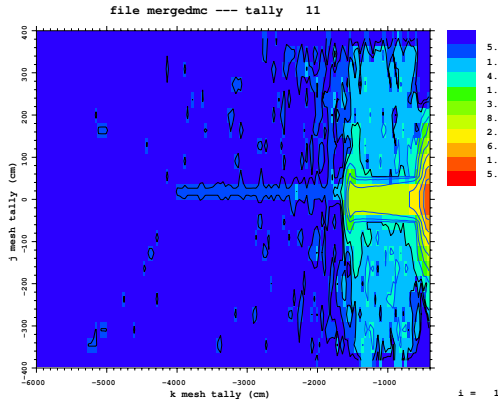


Figure 3: Prompt neutron flux from backscatter.

Prompt Rates from the Beam

Figs. 4 and 5 show the neutron and photon doses due to 1W/m beam losses. The neutron dose is higher than the photon dose peaking at 1.4×10^8 , more typically $10^5 \mu\text{Sv/h}$, as opposed to a peak of 2×10^6 , typically 10^4 . The pattern is similar: in both cases the magnets produce more activity by getting in the way of the escaping beam, rather than shielding from it. Changes to the uniform beam loss distribution did not produce great differences in the dose maps.

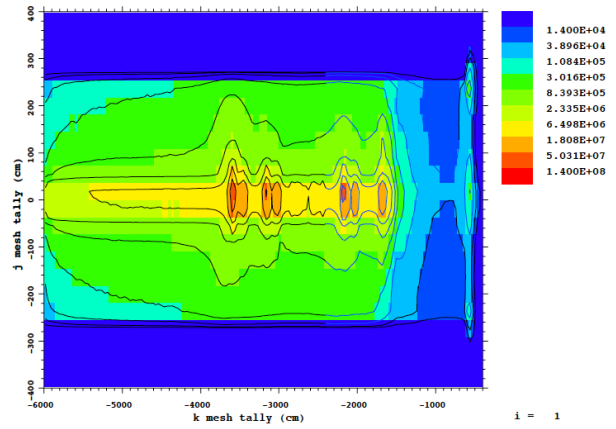


Figure 4: Prompt neutron dose from Beam Loss.

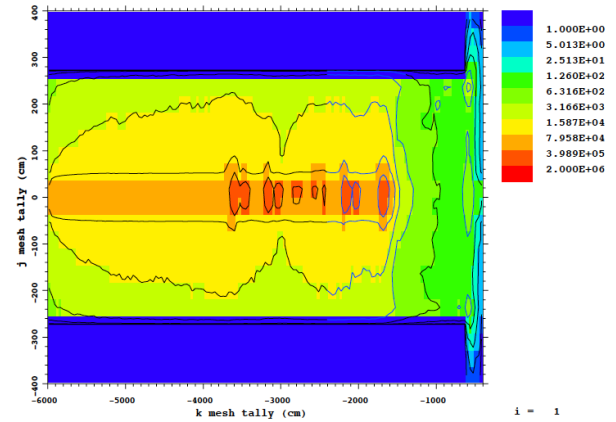


Figure 5: Prompt photon dose from Beam Loss.

We simulate the prompt dose level to which a human body would be exposed by placing a series of notional macrobodies (M), in the form of 30 cm cubes, 115 cm horizontally or vertically from the beam axis. Ten of these sets of 4 (M1 to M10) were placed at the (z) centre position corresponding to the quads and pairs of raster magnets: little difference was seen between values from the four as expected due to the approximate azimuthal symmetry. The results (with the MCNPX fractional error) are shown in Table 2.

Table 2: Prompt Neutron and Photon Dose at Macrobodyes

Macrobody	Centre Position (z) (m)	Neutron Dose ($\mu\text{Sv/h}$)	Photon Dose ($\mu\text{Sv/h}$)
M 1	-35.77	3.2702E+06 0.012	1.4179E+06 0.012
M 2	-34.47	1.6748E+06 0.014	7.6453E+05 0.009
M 3	-31.47	1.5593E+06 0.014	7.1419E+05 0.011
M 4	-30.17	1.1168E+06 0.008	5.3816E+05 0.010
M 5	-27.98	9.3542E+05 0.016	7.5993E+05 0.008
M 6	-26.98	9.4292E+05 0.011	8.2452E+05 0.008
M 7	-25.46	1.0024E+06 0.010	9.5055E+05 0.009
M 8	-24.74	1.0344E+06 0.011	9.4309E+05 0.014
M 9	-21.57	1.8215E+06 0.012	9.0638E+05 0.012
M 10	-20.21	1.2181E+06 0.011	5.9517E+05 0.011

The concrete wall is designed to shield the magnets and accelerator components from the neutron backscatter. The thickness of the concrete wall reduces the effect, as one can

see from Figs. 6 and 7 which show the prompt neutron and photon dose level at M10 (the macrobody placed at the closest quad to the wall). The prompt neutron dose level decreases from 30 Sv/h for 20 cm thickness to 0.15 Sv/h for 200 cm, which is still high. Similarly the prompt photon dose decreases from 13 Sv/h to 0.08 Sv/h.

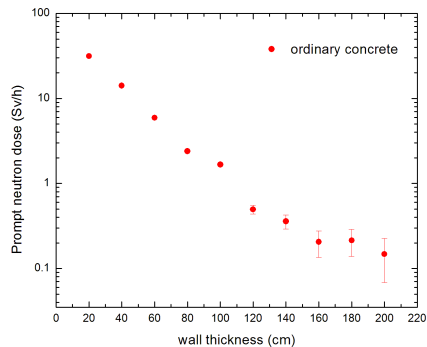


Figure 6: Prompt neutron dose from backsplash.

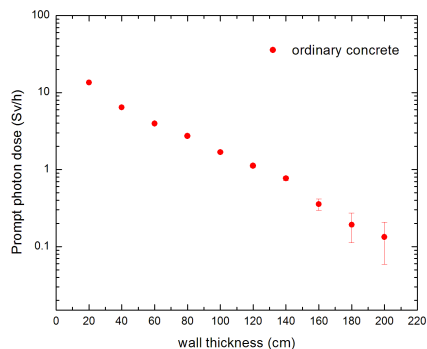


Figure 7: Prompt photon dose from backsplash.

Activation

Over time magnets and accelerator components will require human handling and manipulation. To calculate the dose due to activation involved a two-stage MCNPX process. In the first stages the rate of production R_P for the various isotopes in Table 1 due to beam losses and to backsplash, using the normalisation given earlier, was calculated for individual components. These figures were then used to obtain the decay rate $R_D = R_P(1 - e^{-\lambda t})e^{-\lambda t'}$, where λ is the inverse lifetime of the isotope, t is the nominal running time of 100 days and t' is the resting time of 4 hours. This simple calculation is adequate as multistep decay chains are not involved. These rates were then used to simulate the dose due to photons, with energies as given, produced in the same components using a second-stage MCNPX job with the same geometry deck. Generation occurs uniformly within the component, hence any spatial variation of the activation density within an element is lost in this procedure, but this is not a significant limitation.

For example, the doses due to ^{60}Co produced in the copper of the windings, due to target backsplash (with no shielding wall) and to beam losses are shown in Figs. 8 and 9.

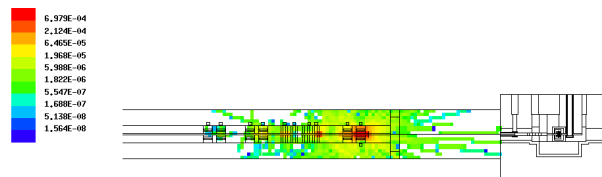


Figure 8: Dose ($\mu\text{Sv/h}$) due to ^{60}Co from backsplash.

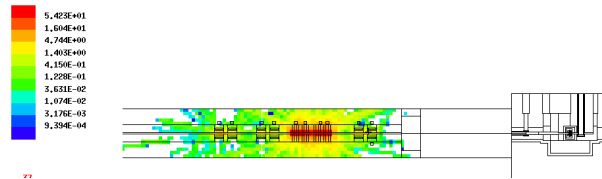


Figure 9: Dose ($\mu\text{Sv/h}$) due to ^{60}Co from beam losses.

The effect of activation due to beam losses is larger than that due to backsplash from the target. This is confirmed by the predictions for macrobodies: the gamma radiation dose at M10 due to beam losses is of the order of $10\mu\text{Sv/h}$ compared to $2.2 \times 10^{-4}\mu\text{Sv/h}$ due to the neutron backsplash.

We have studied the doses produced by the activation of all the isotopes shown in Table 1 with such plots, and also the doses at the macrobodies. For these the largest doses due to beam losses are: ^{60}Co $60\mu\text{Sv/h}$, ^{57}Co $2.25 \times 10^3\mu\text{Sv/h}$, ^{54}Mn and ^{58}Co $0.5\text{--}1\text{ Sv/h}$ and ^{24}Na 65 Sv/h .

Even in the absence of the concrete shielding wall the activation due to neutron backsplash is much lower. At the first quad (M10 macrobody) is registered the highest value, with ^{58}Co showing $1.19 \times 10^4\mu\text{Sv/h}$ and ^{54}Mn $1.23 \times 10^3\mu\text{Sv/h}$. The overall dose is of the order of 0.1mSv/h .

Activation in Air

Activation of air requires a different treatment as the air is circulated. Sullivan [4] quotes a figure of 352 kBq/s/m for 10^{12} particles, averaging neutrons and other hadrons. Alternatively we can calculate the rate of activation caused by the $^{40}\text{Ar}(n, \gamma)^{41}\text{Ar}$ reaction. In both cases the rates appear to be low and acceptable.

CONCLUSION

MCNPX is proving a useful tool for the study of these backgrounds, which can be extended from the beamline region to the instrument hall. Much work remains to be done in verifying these predictions. We are grateful to Riccardo Bevilacqua for helping with MCNPX.

REFERENCES

- [1] S. Peggs (ed.) *ESS Conceptual Design Report* ESS report ESS-2012-001, Lund (2012).
- [2] D B Pelowitz (Ed) *The MCNPX User's Manual*, Version 2.6.0, Report number LA-CP-07-1473 (2008).
- [3] R G Williams *et al.*, *Compendium of Material Composition Data for Radiation Transport Modelling* Report PNNL-15870, Pacific North West Laboratory (2006).
- [4] A H Sullivan, *A guide to radiation and radioactivity levels near high energy particle accelerators*, Nuclear Technology Publishing (1992).